

# Endocannabinoid signal in the gut controls dietary fat intake

Nicholas V. DiPatrizio<sup>a</sup>, Giuseppe Astarita<sup>a,b</sup>, Gary Schwartz<sup>c</sup>, Xiaosong Li<sup>c</sup>, and Daniele Piomelli<sup>a,b,d,1</sup>

<sup>a</sup>Departments of Pharmacology and <sup>d</sup>Biological Chemistry, University of California, Irvine, School of Medicine, Irvine, CA 92697; <sup>b</sup>Unit of Drug Discovery and Development, Italian Institute of Technology, 16163 Genoa, Italy; and <sup>c</sup>Diabetes Research Center, Departments of Medicine and Neuroscience, Albert Einstein College of Medicine of Yeshiva University, Bronx, NY 10461

Edited by Leslie Lars Iversen, University of Oxford, Oxford, United Kingdom, and approved June 6, 2011 (received for review March 23, 2011)

**Oral sensory signals drive dietary fat intake, but the neural mechanisms underlying this process are largely unknown. The endocannabinoid system has gained recent attention for its central and peripheral roles in regulating food intake, energy balance, and reward. Here, we used a sham-feeding paradigm, which isolates orosensory from postingestive influences of foods, to examine whether endocannabinoid signaling participates in the positive feedback control of fat intake. Sham feeding a lipid-based meal stimulated endocannabinoid mobilization in the rat proximal small intestine by altering enzymatic activities that control endocannabinoid metabolism. This effect was abolished by surgical transection of the vagus nerve and was not observed in other peripheral organs or in brain regions that control feeding. Sham feeding of a nutritionally complete liquid meal produced a similar response to that of fat, whereas protein or carbohydrate alone had no such effect. Local infusion of the CB<sub>1</sub>-cannabinoid receptor antagonist, rimonabant, into the duodenum markedly reduced fat sham feeding. Similarly to rimonabant, systemic administration of the peripherally restricted CB<sub>1</sub>-receptor antagonist, URB 447, attenuated sham feeding of lipid. Collectively, the results suggest that the endocannabinoid system in the gut exerts a powerful regulatory control over fat intake and might be a target for antiobesity drugs.**

Mammals have an adaptive advantage in seeking fat-rich foods, which are nutritionally essential but scarce in most natural habitats. This innate preference can become maladaptive, however, when it is not limited by environmental constraints. Indeed, the unrestricted availability of fatty foods, which characterizes diets of industrialized societies, is considered to be a key contributing factor for obesity, diabetes, and cardiovascular disease (1). Despite its theoretical and practical significance, fat preference is still incompletely understood.

In the present study, we examined whether endogenous cannabinoid substances participate in the control of dietary fat intake. The endocannabinoids are a family of biologically active lipids that bind to and activate CB<sub>1</sub>- and CB<sub>2</sub>-cannabinoid receptors, the G protein-coupled receptors targeted by  $\Delta^9$ -tetrahydrocannabinol in *Cannabis*. They include several derivatives of arachidonic acid, which are generated on demand by neurons and other cells in response to physiological or pathological stimuli. The two best-characterized endocannabinoids are 2-arachidonoyl-*sn*-glycerol (2-AG) and anandamide (2). 2-AG is produced through a two-step mechanism in which phospholipase C- $\beta$  activation causes the generation of 1,2-diacylglycerol, which is subsequently cleaved by diacylglycerol lipase- $\alpha$  to yield 2-AG (3). Anandamide production, however, is thought to occur via phospholipase D-mediated hydrolysis of *N*-arachidonoyl phosphatidylethanolamine (4, 5), although alternative pathways have been proposed (6). The biological actions of 2-AG and anandamide are terminated by a combination of facilitated diffusion into cells followed by intracellular enzyme-mediated hydrolysis (2).

The proposed role of endocannabinoids in the hedonic evaluation ("liking") of palatable foods (7, 8) prompted us to ask whether these lipid mediators might be involved in the positive feedback mechanism originating in the mouth, which maintains

fat intake once it has begun (9). For example, recent work has suggested that CB<sub>1</sub>-cannabinoid receptors on the tongue modulate neural activity elicited by a palatable sweet taste (10). Gustatory neural signals from nutrients, including fats and sugars, are transmitted from the oral cavity to the brain via cranial nerves V, VII, IX, and X (11). In particular, cranial nerve X, also termed the vagus nerve, contains branches that communicate efferent and afferent food-related signals between brain and gut (12). To isolate early orosensory signals from subsequent postingestive influences, we used sham feeding in rats, a well-characterized experimental model in which liquid diets are drained from the stomach through a chronically implanted gastric cannula (ref. 9; Fig. S1).

## Results

**Orosensory Properties of Fat Mobilize Small-Intestinal Endocannabinoids.** We allowed rats to sham ingest a corn oil emulsion and measured endocannabinoid content in various brain regions and in peripheral tissues by liquid chromatography/mass spectrometry. Surprisingly, fat sham feeding selectively increased levels of 2-AG and anandamide in the jejunal segment of the gastrointestinal tract (Fig. 1*A* and *B*, 1), but not in other peripheral tissues or brain regions included in our survey (Fig. 2). A similar response was elicited by a nutritionally complete liquid diet (Fig. 1*A* and *B*, 2), whereas sugar (Fig. 1*A* and *B*, 3) or protein solutions were ineffective (Fig. 1*A* and *B*, 4). Irrespective of nutrient composition, sham feeding failed to alter jejunal content of oleoylethanolamide, a lipid-derived satiety factor formed in enterocytes when dietary fat enters the small intestine (ref. 13; Table S1). Notably, severing the vagus nerve below the diaphragm abolished the ability of fat to initiate small-intestinal endocannabinoid production (Fig. S2), which indicates that neural communication from the brain to the gut via the vagus nerve is necessary to drive this biochemical reaction. These findings suggest that cephalic signals elicited by sham feeding of fat, but not other nutrients, selectively mobilize endocannabinoids in the upper gut through a mechanism that is mediated by efferent vagal fibers.

**Sham-Fat Intake Modifies Intestinal Endocannabinoid Metabolism.** Biochemical tests showed that fat sham ingestion enhances jejunal endocannabinoid mobilization through a concerted action on the biosynthesis and degradation of these lipid-derived mediators. Fat sham intake decreased 2-AG-hydrolyzing activity in jejunum (Fig. 3*A*, 1), without influencing activities involved in generating 2-AG (Fig. 3*A*, 2) or its precursor, 1-stearoyl-2-arachidonoyl-*sn*-glycerol (Fig. 3*A*, 3). Moreover, fat sham intake lowered anandamide-hydrolyzing activity (Fig. 3*B*, 1), whereas elevating the activity involved in producing anandamide (Fig. 3*B*,

Author contributions: N.V.D. and D.P. designed research; N.V.D. and X.L. performed research; G.S. and X.L. contributed new reagents/analytic tools; N.V.D., G.A., and D.P. analyzed data; and N.V.D. and D.P. wrote the paper.

The authors declare no conflict of interest.

This article is a PNAS Direct Submission.

<sup>1</sup>To whom correspondence should be addressed. E-mail: piomelli@uci.edu.

This article contains supporting information online at [www.pnas.org/lookup/suppl/doi:10.1073/pnas.1104675108/-DCSupplemental](http://www.pnas.org/lookup/suppl/doi:10.1073/pnas.1104675108/-DCSupplemental).

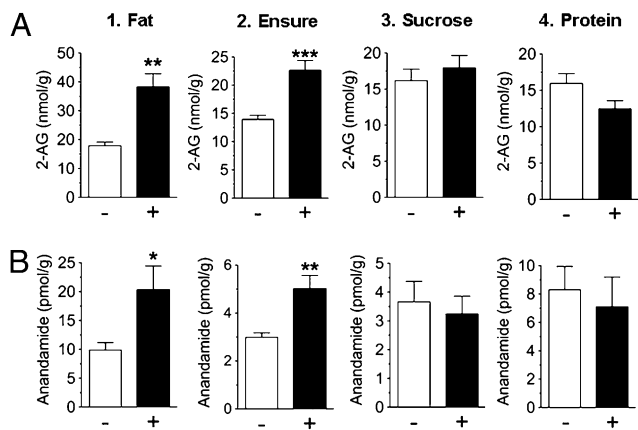


**Fig. 1.** Sham feeding of corn oil or a nutritionally complete liquid diet, but not carbohydrate or protein, mobilize jejunal endocannabinoids. Effects of 30-min sham feeding on levels of jejunal 2-AG (A) and anandamide (B). –, no diet presented; +, diet presented. Results are expressed as mean  $\pm$  SEM;  $n = 5-7$  per condition. Unpaired Student's  $t$  tests, two-tailed, between no diet and diet condition; \* $P < 0.05$ , \*\* $P < 0.01$ , or \*\*\* $P < 0.001$  versus corresponding no diet group.

2) as well as the levels of the anandamide precursor, 1-stearoyl-2-arachidonoyl-*sn*-glycerol-phosphorylethanolamine-*N*-arachidonoyl (Fig. 3B, 3). The enzymes and molecular modifications involved in these effects remain to be determined.

**Intestinal CB<sub>1</sub> Receptors Control Sham Fat Intake.** To examine whether small-intestinal endocannabinoid release regulates fat intake, we measured sham feeding of corn oil while infusing into the rat duodenum an isotonic solution containing the CB<sub>1</sub>-type cannabinoid receptor antagonist/inverse agonist, rimonabant. Intestinal CB<sub>1</sub> receptor blockade caused a dose-dependent inhibition of fat sham intake (Fig. 4A). The high potency of this effect (median effective dose, ED<sub>50</sub>, 0.3 mg·kg<sup>-1</sup>) suggests that intraduodenal rimonabant antagonized endocannabinoid signals elicited in the gut by fat sham ingestion rather than acting at central sites. Two additional findings supported this possibility: First, intraduodenal rimonabant was less potent at reducing normal feeding of standard chow than at decreasing fat sham ingestion (Fig. 4B), and second, systemic administration of the peripherally restricted CB<sub>1</sub>-receptor neutral antagonist, URB447 (14), was also effective at suppressing fat sham intake (Fig. 4C). The latter effect further suggests that pharmacological treatments reduced fat intake by blocking endocannabinoid signaling at CB<sub>1</sub> receptors, rather than inverse agonism of CB<sub>1</sub> receptors, which may have occurred with rimonabant. URB447 displays a weak CB<sub>2</sub>-receptor

**Fig. 2.** Sham feeding of fat fails to affect endocannabinoid levels in other peripheral organs or brain regions. Effects of 30-min sham feeding of corn oil on the levels of 2-AG (Left) and anandamide (Right) in the tongue (Ton), stomach (Stom), ileum, liver, pancreas (Panc), dorsal striatum (Dors), ventral striatum (Vent), lateral regions of the hypothalamus (Lat), medial regions of the hypothalamus (Med), parabrachial nucleus (PBN), and cerebellum (Cere). Open bars, no oil presented; filled bars, oil presented. Results are expressed as mean  $\pm$  SEM;  $n = 5$  per condition; tongue,  $n = 3$  per condition. Two-way repeated measures analysis of variance for brain regions (repeated measure) and diet condition (no oil presented versus oil presented conditions).

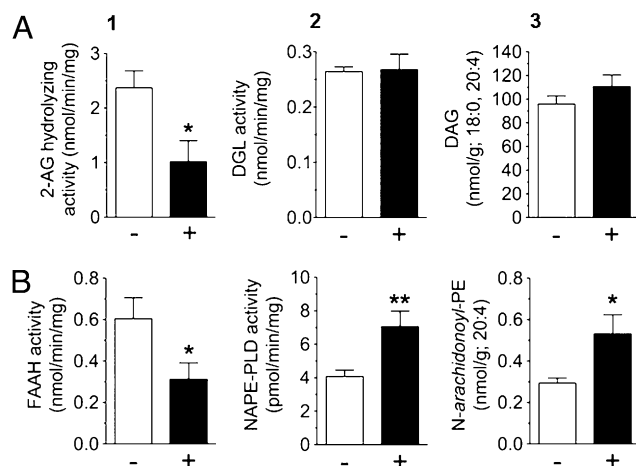
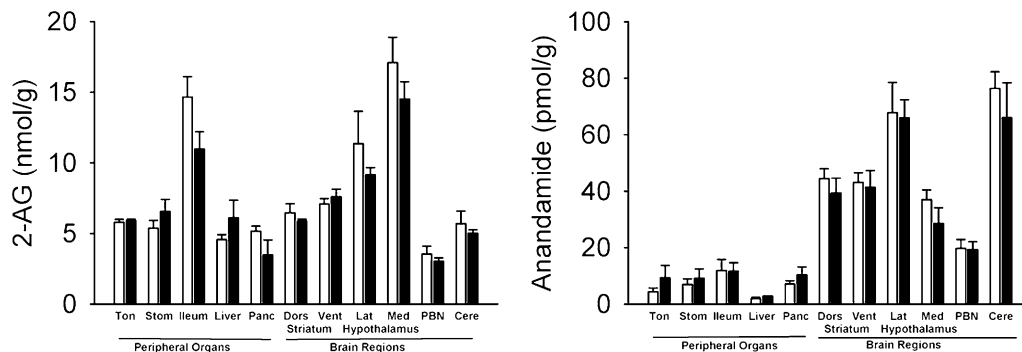


**Fig. 3.** Sham feeding of fat modifies the biosynthesis and degradation of endocannabinoids in the jejunum. Effects of 30-min sham feeding of corn oil on the levels of jejunal 2-AG hydrolysis (A1), biosynthesis (A2), and precursor (A3), and anandamide hydrolysis (B1), biosynthesis (B2), and precursor (B3). –, no diet presented; +, diet presented. Results are expressed as mean  $\pm$  SEM;  $n = 4-5$  per condition. Unpaired Student's  $t$  tests, two-tailed, between no diet and diet condition; \* $P < 0.05$  or \*\* $P < 0.01$  versus corresponding no diet group. DGL, diacylglycerol lipase; DAG, 1-stearoyl-2-arachidonoyl-*sn*-glycerol; FAAH, fatty acid amide hydrolase; NAPE-PLD, *N*-acyl-phosphatidylethanolamine-selective phospholipase D; *N*-arachidonoyl-PE, 1-stearoyl-2-arachidonoyl-*sn*-glycerol-phosphorylethanolamine-*N*-arachidonoyl.

agonist activity in vitro (14); however, systemic treatment with an effective dose of the CB<sub>2</sub>-receptor agonist, JWH-015 (15), failed to modify fat sham intake (Fig. S3). Thus, it is unlikely that URB447 reduced fat intake by acting as an agonist at gut CB<sub>2</sub> receptors. We interpret this set of results to indicate that endocannabinoid signaling at CB<sub>1</sub> receptors in the gut plays an essential role in driving fat sham feeding.

### Discussion

In this work, we have shown that oral exposure to fat stimulates mobilization of the endocannabinoids 2-AG and anandamide in the rat small intestine and that localized functional blockade of this signaling event suppresses fat sham feeding. Our findings identify the gut endocannabinoid system as a critical component of the positive feedback mechanism that drives fat intake and suggest that therapeutic strategies aimed at restraining small-intestinal endocannabinoid activity might help to selectively reduce the overeating of fatty foods.

Previous experiments in rats have shown that the orosensory properties of fat are sufficient to maintain sham intake once it has

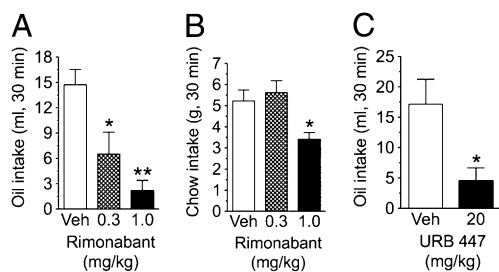


**Fig. 4.** Jejunal endocannabinoids control sham fat intake. Effects of intraduodenal (ID) infusion of rimonabant on 30-min sham feeding of corn oil (A), or normal feeding of chow (B), and i.p. (IP) administration of URB447 (C) on 30-min sham feeding of corn oil. Results are expressed as mean  $\pm$  SEM;  $n = 5-7$  per group. One-way analysis of variance, with a Newman-Keuls post hoc evaluation of means (A and B); paired Student's  $t$  test, two tailed, between vehicle and drug treatment (C); \* $P < 0.05$  or \*\* $P < 0.01$  versus corresponding vehicle treatment.

begun (9) and that oral stimulation is necessary to elicit conditioned place preference to this nutrient (16). Moreover, oral exposure to fat stimulates dopamine outflow in the ventral striatum (17), a brain region that is critical for the evaluation of rewarding sensory stimuli (18). These data support the theory (9) that cephalic-positive feedback mechanisms play a key role in the rewarding properties of fat-rich foods. Our study identifies the intestinal endocannabinoid system as an essential component of this process. Endocannabinoids and their attending cell-surface receptors are found throughout the body and are known to participate in the control of food intake (2, 19). Although much attention has focused on endocannabinoid signaling in the brain (19), the role of peripheral endocannabinoids in food intake is increasingly recognized (20–22). For example, small-intestinal levels of 2-AG and anandamide rise during food deprivation and fall upon refeeding, suggesting that they may signal energy imbalance and promote caloric intake (21, 23). Furthermore, a fat-rich diet modifies intestinal endocannabinoid levels (23, 24). Our studies uncovered an unexpected role for small-intestinal endocannabinoids in controlling the intake of dietary fat driven by oral exposure to this nutrient. Our results, combined with those of prior studies (21, 23), suggest that elevations in intestinal 2-AG and anandamide levels might contribute to the orosensory-mediated induction of fat intake, whereas reductions in the intestinal levels of the same compounds might participate in meal termination. A full test of this hypothesis will require, however, additional experiments.

Based on the present findings, it is reasonable to hypothesize that 2-AG and anandamide act by engaging  $CB_1$  receptors, which are present on enteric neurons and vagal fibers (20), thus modifying the generation or action of neurohumoral factors that affect satiation (meal size) and satiety (intermeal interval), such as ghrelin (25). Although the identification of these factors must await future experimentation, our study does suggest that pharmacological strategies aimed at curbing endocannabinoid activity in the gut might selectively lower the intake of fat-rich foods, a major drive behind overweight and obesity, without affecting reward systems in the brain.

## Materials

**Animals.** Adult male Sprague–Dawley rats (250–300 g) were purchased from Charles River and housed at room temperature (22°C) in individual stainless-steel suspension cages consisting of wire bottoms to prevent coprophagia. Rats were maintained on a 12-h light/dark cycle (on at 0630 hours and off at 1830), and had free access to water and standard chow pellets (Research Diets) throughout the entire study, until two days before testing (see *Test Diets and Feeding Schedule* below for more details). All procedures met the National Institutes of Health guidelines for the care and use

of laboratory animals and were approved by the Institutional Animal Care and Use Committee of the University of California, Irvine.

**Chemicals.** Rimonabant was kindly supplied by the National Institute on Drug Abuse and prepared in 5% propylene glycol, 5% Tween-80, and sterile saline. Rimonabant was administered through intraduodenal (distal) catheters in a volume of 2 mL/kg. URB447 (Cayman Chemical) and JWH-015 (Tocris) were dissolved in 100% DMSO (Sigma-Aldrich) and administered by i.p. injection in a volume of 1 mL/kg. All corresponding vehicle treatments for each compound listed above was administered as described, except no drug was present.

**Test Diets and Feeding Schedule.** Two days before testing, animals began a feeding schedule with free access to standard rodent chow for 6 h (1200–1800 hours). This schedule was maintained daily throughout the duration of testing. Separate groups of animals were sham fed for 30 min (1000–1030 hours) four separate liquid diets: Vanilla Ensure (10 mL; Abbott Nutrition), corn oil emulsion (10 mL at 25% vol/vol; Fisher Scientific), sucrose solution (15 mL at 8% wt/vol; Sigma), or peptone (10 mL at 8% wt/vol; type I enzymatic hydrolysate from meat; Sigma). The concentrations of corn oil, sucrose, and peptone were chosen based on published data indicating that these concentrations are readily sham fed by rats (26–28). The lipid emulsion was prepared (29) by adding an emulsifier (Emplex, 0.4% wt/vol; kindly donated by Caravan Ingredients) to distilled water, followed by heating in a microwave oven for 45 s. An appropriate quantity of corn oil was added to this mixture and homogenized for 5 min by using a rotor-stator homogenizer at 20,000 rpm (Polytron PT 6100). The oil emulsion was allowed to cool on ice for 10 min. All test diets were prepared daily and were at room temperature at the time of presentation to animals.

**Sham-Feeding Procedure.** In the sham-feeding paradigm, nutrients pass through the mouth and esophagus and, subsequently, drain out of the stomach via gastric cannulae (Fig. S1). Extensive prior work with this model has shown that postingestive influences from the diets are removed (9). This work was confirmed experimentally here by showing that fat sham feeding failed to alter jejunal levels of the satiety factor, oleoylethanolamide (Table S1), which is produced when lipids enter the small intestine (13, 30). On test days, animals were placed in individual plastic suspension cages (with a 2-cm wide slit running the entire length of the floor of the cage) one hour (0900) before testing and returned to their metal suspension cages just after completion of testing (1100). The sham-feeding protocol used in this investigation was based on the procedure outlined by G.P. Smith (31). After the 1-h daily acclimation period to the test cages, the stainless-steel plugs were removed from the gastric cannulae, and the stomachs were flushed with saline until the water flowed free of any particles ( $\approx 20$  mL). A stainless-steel tube (1.5 cm in length) was fitted to silastic tubing (25 cm in length, 0.040 inch i. d., 0.085 inch o.d.), threaded into the gastric cannulae, and the tubing placed through the slit in the bottom of the cage allowing the animal to move freely while feeding. Animals were given access to the liquid test diets in small sipper tubes and were allowed to sham feed for 30 min. The liquid diets drained into a plastic container placed just beneath each cage. After the test sessions, the drainage tubes were removed, stomachs were flushed, and the stainless-steel plugs were threaded back into the gastric cannulae. Animals were returned to their home cages and given free access to standard chow for 6 h.

## Methods

**Gastric Cannulae.** The surgical implantation of stainless-steel gastric cannulae into the stomach was performed as described (31). Animals were anesthetized with an i.p. injection of ketamine (100 mg/kg) and xylazine (10 mg/



kg; Western Medical Supply). An incision was made through the skin and abdominal muscle 0.5 cm to the left of midline, and the stomach and spleen were exposed and gently retracted. A 1.0-cm purse-string suture (Nylon Monofilament 4-0 suture; Fisher Scientific) was stitched into the area of cannula placement, then a 5-mm incision was made through the stomach in the middle of the suture. The gastric cannula was inserted into the stomach, and after the tightening of the suture, a second purse-string suture was stitched surrounding the cannula to ensure a tight seal between stomach and cannula. A 1.75-cm circular piece of mylar mesh (to promote growth of tissue for adhesion of stomach to peritoneal wall; Davol) was placed around the base of the cannula, and two small drops of 3M Vetbond skin adhesive (Fisher Scientific) were applied to the mesh for its adhesion to the stomach. The cannulae were externalized through a small incision 1.0 cm to the right of midline. A stainless-steel nut was then threaded onto the cannulae to ensure they remained in proper orientation and externalized. A removable stainless-steel plug was threaded into the cannulae. The abdominal muscle wall was closed by using plain-gut 4-0 suture (Fischer Scientific), and the skin was closed by using stainless-steel wound clips (World Precision Instruments). For pain management, animals were given buprenorphine (0.02 mg/kg i.p.; Western Medical Supply) after completion of surgery. Testing (*Experimental Design*) began after 7–10 d of recovery from surgery.

**Intraduodenal Catheters.** The surgical implantation of catheters was performed as described (13), with a few modifications. Upon completion of externalizing the gastric cannulae (see above), a 2.5-cm silastic tube (0.020 inch i.d., 0.037 inch o.d.; Technical Products Inc. of GA) was inserted, facing toward the distal end of the intestine, and 5 cm distal to the pylorus. This tubing (fabricated before surgery) was fitted 0.5 cm into a slightly larger silastic tube (0.040 inch i.d., 0.085 inch o.d.) with a small piece of mylar mesh surrounding the junction and sealed with silicone adhesive (DAP 100% silicone). After insertion of the smaller tube into the distal duodenum, two small drops of skin adhesive were placed on the mesh to promote adhesion to the intestinal tissue. The larger tube, with an attached (silicone adhesive) circular piece of mesh, was carefully routed up the neck of the animal, exteriorized, then sutured to underlying tissue. A wound clip was placed to close the small opening at the site. The abdominal wall was closed as listed above (*Gastric Cannulae*). A small stainless-steel nail was placed into the end of the catheter. The catheters were flushed with saline (1 mL) daily to prevent occlusion.

**Complete Subdiaphragmatic Vagotomy.** All animals were prepared as detailed above (*Gastric Cannulae*). The stomach and spleen were gently retracted, and before implantation of the gastric cannulae, the dorsal and ventral divisions of the vagus nerve below the diaphragm were isolated with fine forceps and peeled from the esophagus. Two sutures were placed 1.5 cm apart on each division of the vagus (four stitches in total), and all neural tissue between each set of stitches was isolated and removed by using fine scissors. Absence of neural tissue between stitches was used to confirm during tissue collection a full subdiaphragmatic vagotomy. After resection of both branches of the vagus, a gastric cannula was placed in the stomach and the abdominal incision was closed, as described above (*Gastric Cannulae*).

**Brain Tissue.** Brains regions of interest were obtained by hole punch from whole frozen brains mounted in a cryostat (Microm HM525). The following punches were collected, using coordinates from the Paxinos and Watson rat brain atlas (32): dorsal (rostral) or ventral (nucleus accumbens core and shell) striatum (left and right), 2 mm × 2 mm hole punch for each striatal region, from 2.4 to 0.4 mm bregma; lateral regions of the hypothalamus (left and right), 1 mm × 4 mm hole punch, from –0.8 to –4.8 mm bregma; medial regions of the hypothalamus (single punch), 2 mm × 4 mm, from –0.8 to –4.8 mm bregma; parabrachial nucleus (left and right; medial and lateral parabrachial nucleus obtained in each punch), 1 mm × 1 mm hole punch, from –8.8 mm to –9.8 mm bregma; cerebellum (left and right), 1 mm × 1 mm hole punch, from –10.3 mm to –11.3 mm bregma. The punches were placed in individual (per anatomical region) 8-mL glass vials on dry ice, then frozen at –80 °C until time of processing.

**Experimental Design. Influence of the cephalic phase of feeding on endocannabinoid content in brain and peripheral tissues.** Separate groups of animals were sham-fed (30 min, 1000–1030 hours) for four consecutive days (all animals consumed the full amount of liquid diet presented by day four), four separate liquid diets in a small sipper tube: Vanilla Ensure (10 mL); a corn oil emulsion (10 mL); a sucrose solution (15 mL), or a peptone solution (10 mL). On the fifth day of sham feeding, half of each group received the test diet for 30 min, and the other half received an empty sipper tube for 30 min. Immediately after this final 30-min sham-feeding session, animals were anesthetized with iso-fluorane, and peripheral tissues including tongue, stomach, pancreas, liver,

jejunum, and ileum were rapidly removed, rinsed with buffer, and snap-frozen in liquid N<sub>2</sub>. Brains were frozen in methylbutane maintained at –30 °C on dry ice. This method greatly reduces morphological changes that can occur in brains snap-frozen in liquid N<sub>2</sub>. All tissues were subsequently stored at –80 °C until time of processing.

**Effects of CB1 cannabinoid receptor blockade in the proximal-small intestine on sham feeding of fat and real feeding of standard chow.** Animals were maintained on the same daily feeding schedule throughout testing as described above for sham feeding (*Test Diets and Feeding Schedule*), except that each animal was presented with 40 mL of corn oil emulsion. After 4 d of sham feeding (three separate groups of animals), at which time all animals readily consumed at least 10 mL, animals received (day five) a vehicle infusion (intraduodenal) or injection (intraperitoneal) (*Chemicals for Corresponding Vehicle*) 15 min before the sham feeding procedure, and oil intake was recorded for the 30-min test. Twenty-four hours later, each group received rimonabant (intraduodenal infusion, URB447 (IP injection), or JWH-015 (IP injection) (same three separate groups that received their corresponding vehicle, as described above), and fat intake was recorded during the 30-min sham-feeding test. A fourth group of animals was tested for the effects of intraduodenal rimonabant treatment on 30-min normal intake of standard chow. This group was maintained on the same feeding and vehicle/drug-treatment schedule as all other groups listed above. Rimonabant was administered 15 min before their daily presentation of standard chow (1200 hours), and subsequent 30-min intakes of chow were recorded. All animals within all groups received all doses of corresponding drug and vehicle, with at least 72 h separating drug treatments. Within an experimental group, vehicle-treatment intakes for each corresponding drug dose were averaged together for statistical comparison versus drug doses.

**Lipid Extractions.** Frozen tissues were weighed and homogenized in 0.6 mL of methanol containing the following internal standards: [<sup>2</sup>H<sub>4</sub>]-oleoylethanolamide, [<sup>2</sup>H<sub>4</sub>]-anandamide, [<sup>2</sup>H<sub>8</sub>]-2-arachidonoyl-*sn*-glycerol, 1,2-dipalmitoyl-*sn*-glycero-3-phosphoethanolamine-*N*-heptadecanoyl, and dinonadecadienoin (Nu-Chek Prep). Lipids were extracted with chloroform (2 vol) and washed with water (1 vol). Organic phases were collected and fractionated by open-bed silica gel column chromatography, as described (33). Eluted fractions were dried under N<sub>2</sub> and reconstituted in 60 μL of methanol for lipid analyses.

**Fatty Acid Ethanolamides and 2-AG.** We used a 1100 liquid chromatography system coupled to a 1946D-mass spectrometer detector (Agilent Technologies) equipped with an electrospray ionization (ESI) interface. Lipids were separated on a XDB Eclipse C<sub>18</sub> column (50 × 4.6 mm i.d., 1.8 μm, Zorbax), eluted by a gradient of methanol in water (from 85 to 90% methanol in 2.5 min) at a flow rate of 1.5 mL/min. Column temperature was kept at 40 °C. MS detection was in the positive ionization mode, capillary voltage was set at 3 kV, and fragmentor voltage at 120 V. Lipids were quantified with an isotope-dilution method (34) monitoring sodium adducts of the molecular ions [M+Na<sup>+</sup>] in the selected ion-monitoring (SIM) mode.

**N-Acyl Phosphatidylethanolamine (NAPE).** We used a 1100 liquid chromatography system coupled to a XCT Ion Trap MS detector (Agilent Technologies) interfaced with an ESI source. NAPE species were eluted on a Poroshell 300SB C<sub>18</sub> column (2.1 × 75 mm i.d., 5 μm; Agilent) with a linear gradient of methanol in water containing 5 mM ammonium acetate and 0.25% acetic acid (from 85 to 100% in 4 min), at a flow rate of 1 mL/min. NAPE was identified in the negative ionization mode; the capillary voltage was set at –4.5 kV, the skim1 at –40 V, and the capillary exit at –151 V. NAPE was identified by retention time and LC/MS<sup>n</sup> properties as described (32). Extracted ion chromatograms were used to quantify each precursor ion by the following characteristic product ions: 1-stearoyl-2-arachidonoyl-*sn*-glycero-phosphoethanolamine-*N*-arachidonoyl (*m/z* = 1,076.8 > 766.8), and 1,2-dipalmitoyl-*sn*-glycero-3-phosphoethanolamine-*N*-heptadecanoyl (*m/z*=914.8 > 676.6), which was used as an internal standard (35).

**1,2-Diacylglycerol (DAG).** We used an Agilent 1100-LC system coupled to a MS detector Ion-Trap XCT interfaced with ESI (Agilent Technologies). DAG species were separated by using a XDB Eclipse C<sub>18</sub> column (50 × 4.6 mm i.d., 1.8 μm; Zorbax), eluted by a gradient of methanol in water (from 85 to 90% methanol in 2.5 min) at a flow rate of 1.5 mL/min. Column temperature was kept at 40 °C. The capillary voltage was set at 4.0 kV and skimmer voltage at 40 V. N<sub>2</sub> was used as drying gas at a flow rate of 12 L/min, temperature at 350 °C, and nebulizer pressure at 80 psi. Helium was used as collision gas, and fragmentation amplitude was set at 1.2 V. DAG were identified in the positive ionization mode based on their retention times and MS<sup>3</sup> properties, using synthetic standards as references. Multiple reaction monitoring was

used to acquire full-scan tandem MS spectra of selected DAG ions. Extracted ion chromatograms were used to quantify 1-stearoyl,2-arachidonoyl-*sn*-glycerol ( $m/z = 667.8 > 341.5$ ) and dinonadecadienoin ( $m/z = 667.8 > 367.5$ ), which was used as an internal standard.

***N*-Arachidonoyl Phosphatidylethanolamine-Specific Phospholipase D Activity.** Jejunal tissue was homogenized in ice-cold Tris-HCl (50 mM at pH 7.5, 10 vol) containing 0.32 M sucrose. Homogenates were centrifuged at  $1,000 \times g$  for 10 min and supernatants (0.1 mg of protein) were incubated at 37 °C for 30 min in Tris-HCl (50 mM at pH 7.4, 0.2 mL) containing 0.1% Triton X-100, phenylmethylsulfonyl fluoride (1 mM) and 1,2-dipalmitoyl-*sn*-glycero-3-phosphoethanolamine-*N*-heptadecenoyl (0.1 mM). Reactions were stopped by adding 0.6 mL of chloroform-methanol (1:1, vol/vol) containing *N*-heptadecenoyl- $[^2\text{H}_4]$ -ethanolamide ( $m/z = 338$ ) as internal standard. After centrifugation at  $1,000 \times g$  at 4 °C for 10 min, the organic layers were collected and dried under  $\text{N}_2$ . The residues were suspended in 50  $\mu\text{L}$  of chloroform/methanol (1:3, vol/vol) and analyzed by LC/MS. We quantified *N*-heptadecenoyl ethanolamide ( $m/z = 334$ ) with an isotope-dilution method, monitoring sodium adducts of molecular ions in the SIM mode (35).

**Fatty Acid Amide Hydrolase Activity.** Jejunal tissue was homogenized and homogenates were centrifuged at  $1,000 \times g$  for 10 min. Supernatants (50  $\mu\text{g}$  of protein) were incubated with  $[^3\text{H}]$ -anandamide (arachidonoyl  $[^3\text{H}]$ -ethanolamine; 10,000 dpm, specific activity 20 Ci/mmol) for 30 min at 37 °C in 0.5 mL of 50 mM Tris-HCl buffer (pH 8.0) containing fatty acid-free BSA (0.05% weight/vol). Reactions were terminated adding 1.5 mL of chloroform/methanol (2:1, vol/vol), and phases were separated by centrifugation. The aqueous layers were collected, and  $[^3\text{H}]$ -ethanolamine was quantified by liquid scintillation counting.

**DAG Lipase Activity.** Jejunal tissue was homogenized in ice-cold Tris-HCl (50 mM, pH 7.5, 10 vol) containing 0.32 M sucrose. Homogenates were centrifuged at  $1,000 \times g$  for 10 min, and the supernatants (0.1 mg of protein) were in-

cubated at 37 °C for 30 min in Tris-HCl (50 mM, pH 7.5, 0.2 mL) containing 0.1% Triton X-100, and diheptadecenoin (50  $\mu\text{M}$ ). Reactions were stopped by adding 0.6 mL of chloroform-methanol (2:1, vol/vol) containing  $[^2\text{H}_8]$ -2-AG ( $m/z = 409$ ) as an internal standard. After centrifugation at  $1,000 \times g$  at 4 °C for 10 min, the organic layers were collected and dried under  $\text{N}_2$ . The residues were suspended in 60  $\mu\text{L}$  of chloroform/methanol (1:3, vol/vol) and analyzed by LC/MS. We quantified monoheptadecenoin ( $m/z = 365$ ) with an isotope-dilution method, monitoring sodium adducts of molecular ions in the SIM mode (36).

**2-AG Hydrolyzing activity.** Jejunal tissue was homogenized in ice-cold Tris-HCl (50 mM, pH 7.5, 10 vol) containing 0.32 M sucrose. Homogenates were centrifuged at  $1,000 \times g$  for 10 min, and the supernatants (0.1 mg protein) were incubated at 37 °C for 30 min in Tris-HCl (50 mM, pH 7.4, 0.5 mL) containing 0.05% BSA, and monoheptadecenoyl glycerol (10  $\mu\text{M}$ ). Reactions were stopped by adding 0.6 mL of chloroform-methanol (2:1, vol/vol) containing heptadecanoic acid ( $m/z = 269$ ) as internal standard. After centrifugation at  $1,000 \times g$  at 4 °C for 10 min, the organic layers were collected and dried under  $\text{N}_2$ . The residues were suspended in 60  $\mu\text{L}$  of chloroform/methanol (1:3, vol/vol) and analyzed by LC/MS. We quantified heptadecanoic acid ( $m/z = 267$ ) with an isotope-dilution method, monitoring pseudomolecular ions in the SIM mode (37).

**Statistical Analyses.** Results are expressed as the mean  $\pm$  SEM. The significance of differences between groups was evaluated by Student's *t* test, or a one- or two-way analysis of variance (ANOVA) followed by a Newman-Keuls post hoc evaluation for comparison of means when significant differences were found. Analyses were made by using GraphPad Prism software (GraphPad Software), and differences were considered significant if  $P < 0.05$ .

**ACKNOWLEDGMENTS.** We like thank Ashley Shibuya, Milad Danesh, David Grigoryan as well as Drs. Jin Fu, Kwang-Mook Jung, Ana Gujjarro, and Jason Clapper for help with experiments. This work was supported by National Institutes of Health Grants DK073955, DA012413, and 1RL1AA017538 (to D.P.).

- Cordain L, et al. (2005) Origins and evolution of the Western diet: Health implications for the 21st century. *Am J Clin Nutr* 81:341–354.
- Piomelli D (2003) The molecular logic of endocannabinoid signalling. *Nat Rev Neurosci* 4:873–884.
- Stella N, Schweitzer P, Piomelli D (1997) A second endogenous cannabinoid that modulates long-term potentiation. *Nature* 388:773–778.
- Di Marzo V, et al. (1994) Formation and inactivation of endogenous cannabinoid anandamide in central neurons. *Nature* 372:686–691.
- Cadas H, Gaillet S, Beltramo M, Venance L, Piomelli D (1996) Biosynthesis of an endogenous cannabinoid precursor in neurons and its control by calcium and cAMP. *J Neurosci* 16:3934–3942.
- De Petrocellis L, Di Marzo V (2009) An introduction to the endocannabinoid system: From the early to the latest concepts. *Best Pract Res Clin Endocrinol Metab* 23:1–15.
- Mahler SV, Smith KS, Berridge KC (2007) Endocannabinoid hedonic hotspot for sensory pleasure: Anandamide in nucleus accumbens shell enhances 'liking' of a sweet reward. *Neuropsychopharmacology* 32:2267–2278.
- DiPatrizio NV, Simansky KJ (2008) Activating parabrachial cannabinoid CB1 receptors selectively stimulates feeding of palatable foods in rats. *J Neurosci* 28:9702–9709.
- Greenberg D, Smith GP (1996) The controls of fat intake. *Psychosom Med* 58:559–569.
- Yoshida R, et al. (2010) Endocannabinoids selectively enhance sweet taste. *Proc Natl Acad Sci USA* 107:935–939.
- Hamilton RB, Norgren R (1984) Central projections of gustatory nerves in the rat. *J Comp Neurol* 222:560–577.
- Berthoud HR (2008) The vagus nerve, food intake and obesity. *Regul Pept* 149:15–25.
- Schwartz GJ, et al. (2008) The lipid messenger OEA links dietary fat intake to satiety. *Cell Metab* 8:281–288.
- LoVerme J, et al. (2009) Synthesis and characterization of a peripherally restricted CB1 cannabinoid antagonist, URB447, that reduces feeding and body-weight gain in mice. *Bioorg Med Chem Lett* 19:639–643.
- Torres E, et al. (2011) Evidence that MDMA ('ecstasy') increases cannabinoid CB2 receptor expression in microglial cells: Role in the neuroinflammatory response in rat brain. *J Neurochem* 113:67–78.
- Suzuki A, Yamane T, Imaizumi M, Fushiki T (2003) Integration of orosensory and postingestive stimuli for the control of excessive fat intake in mice. *Nutrition* 19:36–40.
- Liang NC, Hajnal A, Norgren R (2006) Sham feeding corn oil increases accumbens dopamine in the rat. *Am J Physiol Regul Integr Comp Physiol* 291:R1236–R1239.
- Kelley AE (2004) Ventral striatal control of appetitive motivation: Role in ingestive behavior and reward-related learning. *Neurosci Biobehav Rev* 27:765–776.
- Di Marzo V, Ligresti A, Cristino L (2009) The endocannabinoid system as a link between homeostatic and hedonic pathways involved in energy balance regulation. *Int J Obes (Lond)* 33(Suppl 2):S18–S24.
- Izzo AA, Sharkey KA (2010) Cannabinoids and the gut: New developments and emerging concepts. *Pharmacol Ther* 126:21–38.
- Gómez R, et al. (2002) A peripheral mechanism for CB1 cannabinoid receptor-dependent modulation of feeding. *J Neurosci* 22:9612–9617.
- Cluny NL, et al. (2010) A novel peripherally restricted cannabinoid receptor antagonist, AM6545, reduces food intake and body weight, but does not cause malaise, in rodents. *Br J Pharmacol* 161:629–642.
- Izzo AA, et al. (2009) Peripheral endocannabinoid dysregulation in obesity: Relation to intestinal motility and energy processing induced by food deprivation and re-feeding. *Br J Pharmacol* 158:451–461.
- Artmann A, et al. (2008) Influence of dietary fatty acids on endocannabinoid and *N*-acylethanolamine levels in rat brain, liver and small intestine. *Biochim Biophys Acta* 1781:200–212.
- Al-Massadi O, et al. (2011) Peripheral endocannabinoid system-mediated actions of rimonabant on growth hormone secretion are ghrelin-dependent. *J Neuroendocrinol* 22:1127–1136.
- Darcel NP, Liou AP, Tomé D, Raybould HE (2005) Activation of vagal afferents in the rat duodenum by protein digests requires PepT1. *J Nutr* 135:1491–1495.
- Mindell S, Smith GP, Greenberg D (1990) Corn oil and mineral oil stimulate sham feeding in rats. *Physiol Behav* 48:283–287.
- Nissenbaum JW, Sclafani A (1987) Sham-feeding response of rats to Polycose and sucrose. *Neurosci Biobehav Rev* 11:215–222.
- Touzani K, Sclafani A (2001) Conditioned flavor preference and aversion: Role of the lateral hypothalamus. *Behav Neurosci* 115:84–93.
- Rodríguez de Fonseca F, et al. (2001) An anorexic lipid mediator regulated by feeding. *Nature* 414:209–212.
- Smith GP (2001) Sham feeding in rats with chronic, reversible gastric fistulas. *Curr Protoc Neurosci* Chap 8:Unit 8.6D.
- Paxinos G, Watson C (1998) *The rat brain in stereotaxic coordinates* (Academic, San Diego).
- Astarita G, Piomelli D (2009) Lipidomic analysis of endocannabinoid metabolism in biological samples. *J Chromatogr B Analyt Technol Biomed Life Sci* 877:2755–2767.
- Giuffrida A, Rodríguez de Fonseca F, Piomelli D (2000) Quantification of bioactive acylethanolamides in rat plasma by electrospray mass spectrometry. *Anal Biochem* 280:87–93.
- Fu J, et al. (2007) Food intake regulates oleoylethanolamide formation and degradation in the proximal small intestine. *J Biol Chem* 282:1518–1528.
- Jung KM, et al. (2007) A key role for diacylglycerol lipase- $\alpha$  in metabotropic glutamate receptor-dependent endocannabinoid mobilization. *Mol Pharmacol* 72:612–621.
- King AR, et al. (2007) URB602 inhibits monoacylglycerol lipase and selectively blocks 2-arachidonoylglycerol degradation in intact brain slices. *Chem Biol* 14:1357–1365.